

Surface nanostructuring by bichromatic femtosecond laser pulses through a colloidal particle array

N.M. Bityurin, A.V. Afanasiev, V.I. Bredikhin, A.V. Pikulin, I.E. Ilyakov, B.V. Shishkin, R.A. Akhmedzhanov, E.N. Gorshkova

Abstract. This paper considers the surface nanostructuring of polymers and glasses by femtosecond laser pulses using an array of colloidal particles as a focusing system. We demonstrate that partial conversion of the femtosecond laser pulse energy into the second harmonic considerably reduces the surface modification threshold and the size of the resulting structural elements. At intensities above 10^{12} W cm⁻², surface modification (ablation and swelling) occurs through free carrier generation. In this process, the second harmonic is more efficient in multiphoton ionisation, whereas the fundamental is more efficient in impact ionisation. The second harmonic is better focused by colloidal particle arrays than is the fundamental. As a result, the use of bichromatic pulses ensures a decrease in both the surface modification threshold and the size of the resulting structural elements. We discuss the optical properties of colloidal particle arrays and the ways of producing such arrays on dielectric substrates.

Keywords: femtosecond pulses, second harmonic, bichromatic light, surface nanostructuring, colloidal particle arrays.

1. Introduction

In producing individual nanofeatures on solid surfaces, laser technologies can hardly compete with methods that employ electron beams. At the same time, nanostructuring by laser radiation has significant advantages in producing large-area arrays of structures. There are two main approaches to large-area surface nanostructuring by laser radiation: the use of laser beam interference and structuring with the use of near-field masks. The latter approach is preferable for modifying solid surfaces by femtosecond laser pulses because of the weak interference of such pulses on large areas. The simplest type of near-field mask is an array of dielectric microparticles. Such arrays are commonly produced on solid surfaces by deposition from colloidal solution and become close-packed through self-organisation processes. Colloidal particle arrays

on solid surfaces are used for surface nanostructuring by laser radiation. This surface nanomodification process (sometimes referred to as laser nanosphere lithography) has been the subject of extensive studies [1–9].

In addition, there is much discussion whether the efficiency of the action of a femtosecond laser pulse on matter can be increased by varying the pulse shape through spectral phase modulation [10–12]. The high-frequency part of a pulse is then located at its leading edge, ensuring efficient multiphoton ionisation, whereas the low-frequency part is quite effective for impact ionisation. It is worth pointing out however that, in a previous study [13], this idea was realised not for the high- and low-frequency parts of a femtosecond pulse but for the second harmonic (SH) and fundamental frequency (FF), which appears more efficient. Thus, the SH produces seed electrons and the fundamental ensures an energy effect. In this study, surfaces have been exposed to bichromatic light through a focusing system consisting of colloidal particles.

2. Optics of colloidal particle arrays

In near-field lithography, transparent dielectric microspheres are employed as microlenses to focus incident laser radiation. Microsphere arrays are produced directly on a substrate to be structured. Under laser irradiation, each microsphere creates a local laser field amplification region in the substrate directly under it. As a result, periodic structures can be produced on the substrate. Note that the spheres are not independent individual microlenses in a close-packed array: a significant role can be played by light rescattering between neighbouring microspheres, and various collective effects are possible.

At present, several phenomena due to the coupling of spheres in close-packed colloidal arrays and important for laser micro- and nanostructuring are known. Pikulin et al. [6] studied structures produced by femtosecond laser pulses incident on an array of dielectric spheres half of which had been coated with gold by sputter deposition. In a number of instances, the laser exposure led to the formation of hexagonal apertures in the gold coating. The generation of such structures was interpreted in terms of the laser field distribution, related to collective effects in the sphere array. Wang et al. [14] studied ablation of a material by laser radiation focused by an array of spheres on the surface to be modified. The ablation nanocraters under the spheres located at the boundary of the array were found to be deeper. Calculation of the laser field distribution revealed energy flows in the colloidal particle array from the inner to outer spheres,

N.M. Bityurin, A.V. Afanasiev, V.I. Bredikhin, A.V. Pikulin, I.E. Ilyakov, B.V. Shishkin, R.A. Akhmedzhanov Institute of Applied Physics, Russian Academy of Sciences, ul. Ul'yanova 46, 603950 Nizhnii Novgorod, Russia;
e-mail: bit@appl.sci-nnov.ru, ava@ufp.appl.sci-nnov.ru;
E.N. Gorshkova N.I. Lobachevsky Nizhnii Novgorod State University, prosp. Gagarina 23, 603950 Nizhnii Novgorod, Russia

Received 3 March 2014; revision received 17 March 2014
Kvantovaya Elektronika 44 (6) 556–562 (2014)
Translated by O.M. Tsarev

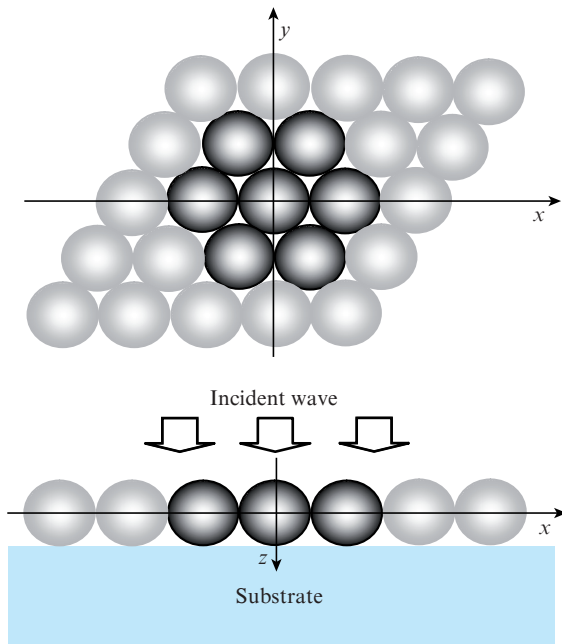


Figure 1. Part of an infinite monolayer of microspheres on a substrate (darker circles represent a cluster of seven spheres).

resulting in a stronger near field near the latter spheres. Pikulin et al. [7] demonstrated elongation of the focal volume behind a sphere due to the effect of its neighbours, which may cause an order of magnitude change in the height of the resulting convex structures [9]. It is necessary to find and investigate such effects for the ability to effectively employ microsphere arrays as near-field focusing devices for nanostructuring.

Below, we present calculated distributions of the square of the electric field amplitude, $|E|^2$, for various configurations of polystyrene spheres on a glass substrate: a single sphere, a close-packed hexagonal cluster of seven spheres and an infinite close-packed monolayer. The arrangement of the spheres is shown schematically in Fig. 1. Calculations were made for the spheres exposed to a bichromatic plane wave at wavelengths of 800 (FF of the Ti:sapphire laser) and 400 nm (SH). The calculation results in Fig. 2 indicate that the SH is better focused by the spheres than is the fundamental. Moreover, for both the spheres in the finite cluster and the infinite monolayer, collective phenomena have a marked influence on focusing, reducing the intensity and leading to the formation of a long focus.

The calculations were performed by a finite-difference time-domain (FDTD) method at a grid size of 10 nm. To simulate an infinite monolayer of spheres, we used periodic boundary conditions along the x and y axes. In the other cases, a perfectly matched layer (PML) 0.4 to 1 μm in thickness was utilised to suppress edge effects at the boundaries of the computational mesh.

3. Preparation of a colloidal particle array on a solid surface

Current views of the nature of colloidal crystals originate from Langmuir's work [15], which addressed the interaction between colloidal particles in solution and on solid surfaces and identified conditions for the formation of colloidal crystals. In particular, Langmuir highlighted the important role of the dielectric permittivity of the solvent. In addition, he proposed an experimental method for producing layers of close-packed particles on solid surfaces (2D colloidal crystals) through pulling of colloidal solution onto a substrate by virtue of surface tension and concurrent drying of the

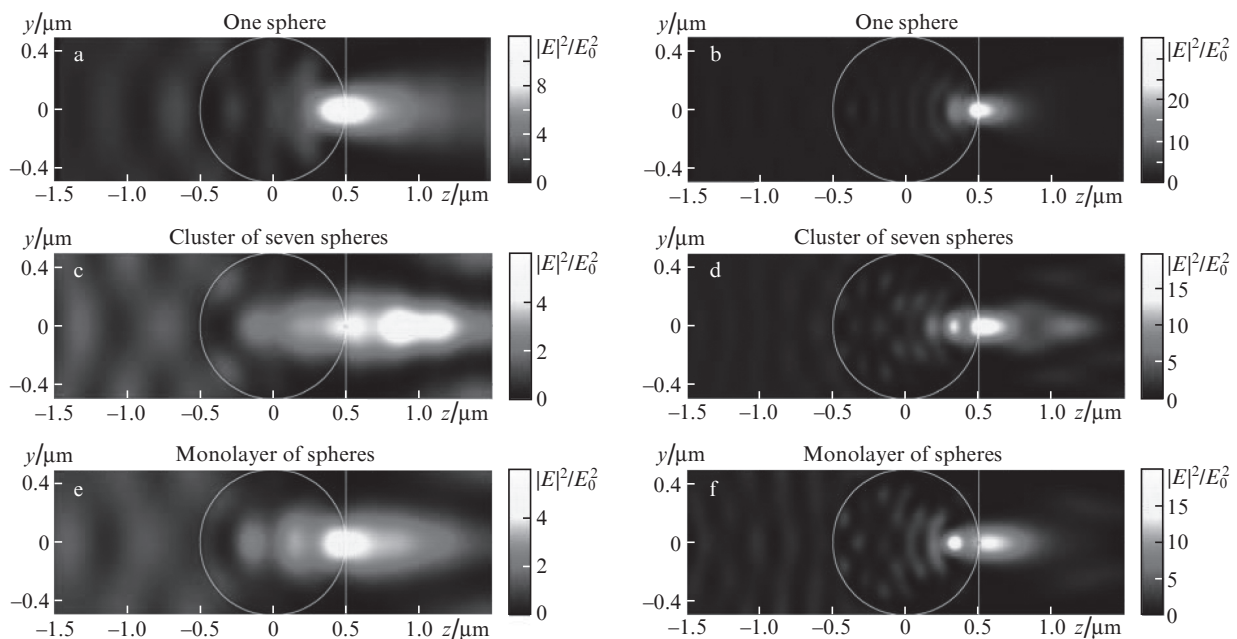


Figure 2. $|E|^2$ distributions near 1- μm -diameter polystyrene spheres ($n = 1.59$) on a glass substrate ($n = 1.46$) under the action of a normally incident plane wave linearly polarised along the x coordinate; $\lambda =$ (a, c, e) 800 and (b, d, f) 400 nm. The distributions are normalised to the field in the incident wave.

resulting layer [16, 17]. Subsequently, various versions of the Langmuir–Blodgett method were proposed with the aim of preparing large-area perfect 2D colloidal crystals [18]. In recent years, the advent of nanosphere lithography, including laser nanosphere lithography, has renewed interest in this area of research, because a need has emerged for methods of producing high-quality colloidal crystals from elements of various origins, shapes and dimensions on various types of substrates. One ‘popular’ system is a colloidal crystal from micron- or submicron-sized transparent (SiO_2 or polystyrene) spheres, which can be used as focusing microlenses e.g. in laser nanolithography. Despite the large number of reports in this area of research (see e.g. the above-mentioned review [18]), the ability to produce high-quality large-area two-dimensional colloidal single crystals remains a challenge. This is particularly so in the case of polymer substrates. The difficulty is that water (offering the advantage of high dielectric permittivity) is often used as a solvent in colloidal solutions, but polymers are typically hydrophobic. Meanwhile, the ability to produce colloidal crystals on polymers is an important issue, because some polymers are used as resists and others are potentially attractive for micro- and optoelectronic applications.

Khan et al. [4] proposed using adhesive tape to transfer a colloidal monolayer from the surface of liquid to a sample, but the presence of an additional outer layer limits the utility of such coatings.

In this study, microparticle arrays on a polymer (PMMA) surface were produced via the preparation of a suspension of particles in a complex solvent directly on the surface. On the one hand, this reduced the dielectric permittivity of the solvent and, hence, increased the probability of stray aggregation. On the other, this improved the wettability of the substrate surface. By optimising the solvent composition, it is possible to obtain microparticle arrays on a polymer which are perfect enough for laser irradiation experiments described below.

Polystyrene spheres $\sim 1 \mu\text{m}$ in diameter (mean deviation of the diameter within $0.06 \mu\text{m}$) were applied to PMMA and glass substrates. As glass substrates, we used microscope slides (ApexLab Co.). A suspension with a particular concentration of spheres was prepared so that drying a droplet of the

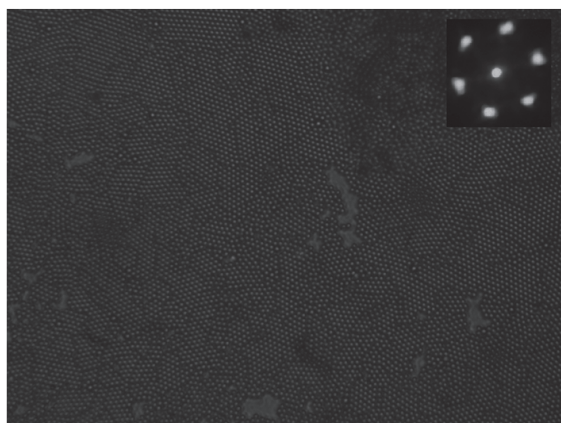


Figure 3. Microphotograph of a monolayer of polystyrene spheres $\sim 1 \mu\text{m}$ in diameter on PMMA. Inset: diffraction pattern obtained by exposing the monolayer to a probe laser beam with $\lambda = 532 \text{ nm}$.

suspension on the surface of a substrate produced a close-packed hexagonal monolayer. Structural defects and the domain size in such layers were determined by the statistical dispersion in the sphere size. Each close-packed domain consisted of hundreds of microparticles. Figure 3 is a micrograph of a monolayer of polystyrene spheres on PMMA.

We used diffraction of a cw laser beam from the layers (Fig. 3) to rapidly assess their structural perfection. A hexagonal structure of the diffracted beam indicated that the probe laser beam spot included a region of the microparticle array suitable for use.

4. Effect of femtosecond laser pulses

Below, we consider the surface nanostructuring of a dielectric by exposing it to harmonics of single femtosecond Ti:sapphire laser pulses.

In our experiments, we used a Spectra-Physics Spitfire Pro laser operated in single-shot mode (the experimental setup is shown schematically in Fig. 4). The pulse duration was 50 fs, the pulse energy was 1.7 mJ, the centre wavelength was 800 nm, and the beam diameter was 7 mm. The beam was focused by a flat–convex lens with a focal length of 15 cm. We investigated the formation of periodic nanostructures consisting of ablation craters or hillocks under various laser irradiation conditions. Samples were exposed to single femtosecond laser pulses at the FF, SH pulses and bichromatic (FF + SH) pulses. A thin ($100 \mu\text{m}$) BBO crystal (type II phase matching: ooe) was used for SH generation with a maximum integrated efficiency of 5%. The crystal orientation was varied to change the conversion efficiency (phase matching). To avoid temporal separation of the FF and SH pulses, the crystal was placed behind the lens. A 3-mm-thick blue glass filter (with absorbances $A_{400} < 0.02$ and $A_{800} > 20$) was used to separate the SH. The fluence in the laser spot was varied by moving the

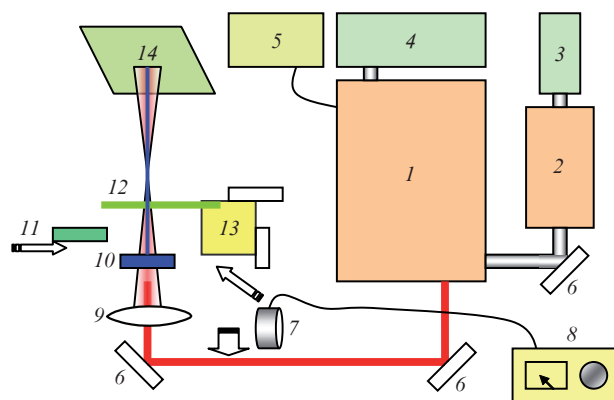


Figure 4. Optical layout of the experimental setup (50-fs pulses with a centre wavelength of 800 nm; beam diameter, 7 mm): (1) Spitfire 50 FS femtosecond laser system (Spectra-Physics); (2) master oscillator of the femtosecond system (Tsunami); (3) pump laser of the master oscillator (Millennia); (4) pump laser of the Spitfire amplifier (Empower); (5) personal computer controlling the lasing mode (single-shot mode or 1-kHz pulse repetition rate); (6) high-reflectivity mirrors; (7) detector of an optical power meter; (8) optical power meter; (9) lens ($F = 15 \text{ cm}$); (10) thin BBO crystal for SHG; (11) glue glass (SZS-21) filter for SH separation; (12) sample (microspheres on a glass or PMMA plate) on a multi-axis translation stage; (13) translation stage; (14) screen.

sample along the axis of the focused beam. The sample was located much closer to the lens than was the air breakdown region. Hereafter, the fluence of a bichromatic pulse is taken to mean the fluence of the FF pulse before the orientation of the BBO crystal was adjusted to correspond to the phase matching condition.

In surface analysis, we used an atomic force microscope. The best imaging quality was achieved in intermittent contact mode.

5. Results and discussion

When the laser pulse fluence was just above a certain threshold (threshold intensity of $5 \times 10^{11} \text{ W cm}^{-2}$ for a bichromatic pulse and $10^{12} \text{ W cm}^{-2}$ for an FF pulse), the spheres were swept away from the irradiated surface area. The process was similar to laser cleaning [19]. When the fluence exceeded the laser cleaning threshold by 15%, we obtained ablation craters on the PMMA substrates and hillocks on the glass substrates (Figs 5, 6). In the case of the glass substrates, the sphere removal threshold and, accordingly, the structuring onset fluence for a bichromatic beam were about half those for an FF beam. In the case of the PMMA substrates, the distinction was even greater. In both instances, the pulse fluence needed

for structuring by a bichromatic pulse was substantially lower than that needed for laser cleaning by an FF pulse.

The addition of the SH leads to the formation of more localised ablation craters, $\sim 100 \text{ nm}$ in diameter, on the PMMA substrates. Statistical processing results (Fig. 7) indicate that the pits produced on PMMA by bichromatic and SH pulses differ little in diameter and are smaller than the pits produced by FF pulses.

If the FF component was filtered off and only the SH was used, structuring occurred only when the sample was placed much closer to the focus of the beam than in the case of structuring under the action of a bichromatic pulse. Displacement of the sample led to an increase in incident intensity. Even with the absorption in the filter taken into account, the threshold SH fluence was several times the SH partial fluence in the bichromatic beam near the structuring threshold. The dispersion-induced pulse broadening in the filter, which reduced the peak intensity by less than 30%, had no critical influence. This means that the FF component of the bichromatic pulse made an appreciable contribution to surface modification. We assume that the surface modification was due to charge carrier (plasma) generation. In what follows, in examining carrier generation mechanisms this process will be referred to as ionisation, as is common in

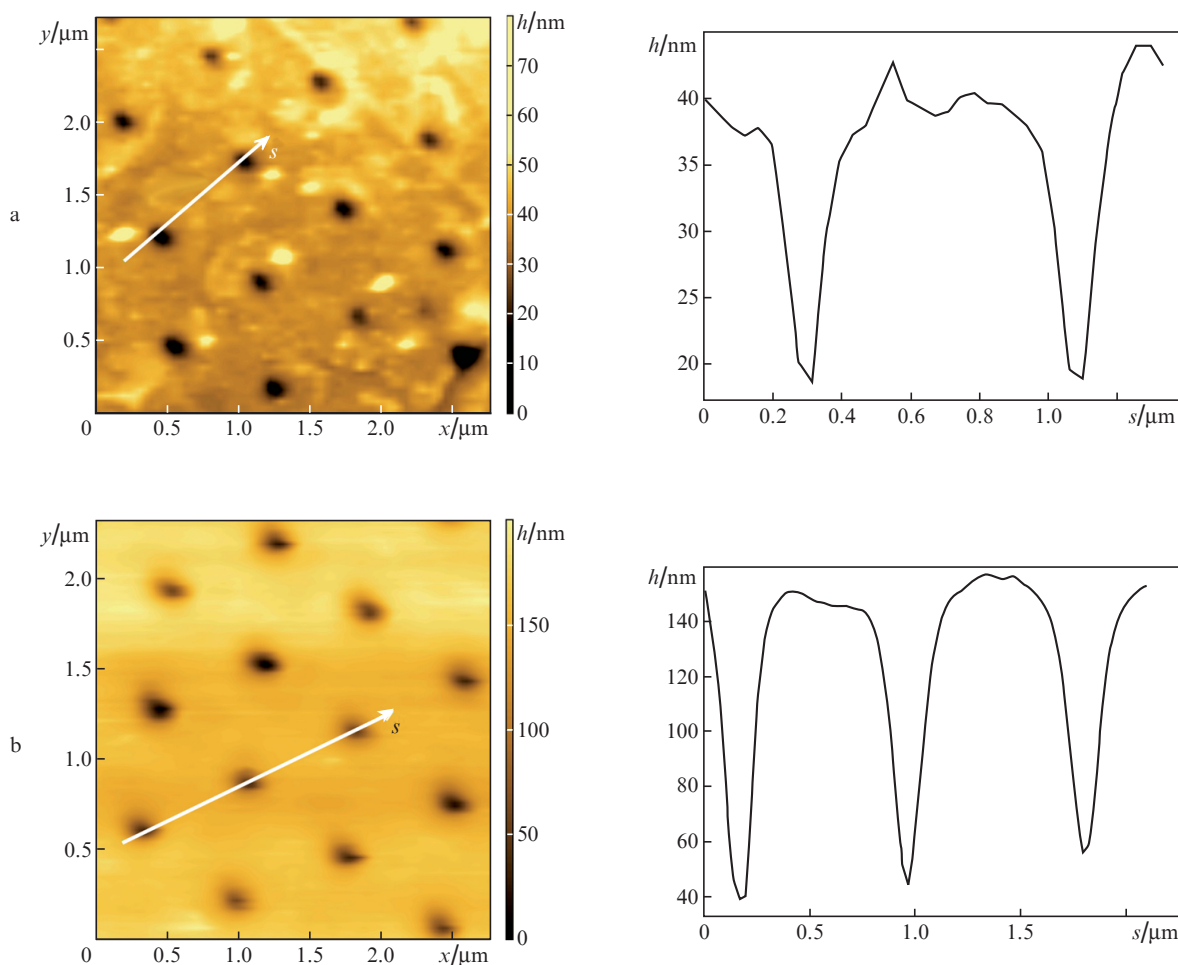


Figure 5. Structures (ablation craters) obtained on PMMA by exposure to a single femtosecond pulse through a microsphere array: (a) bichromatic pulse, (b) SH pulse. Shown in the right panels are the height profiles along lines s in the colour maps of the height (h) distributions above the xy plane (atomic force microscope images).

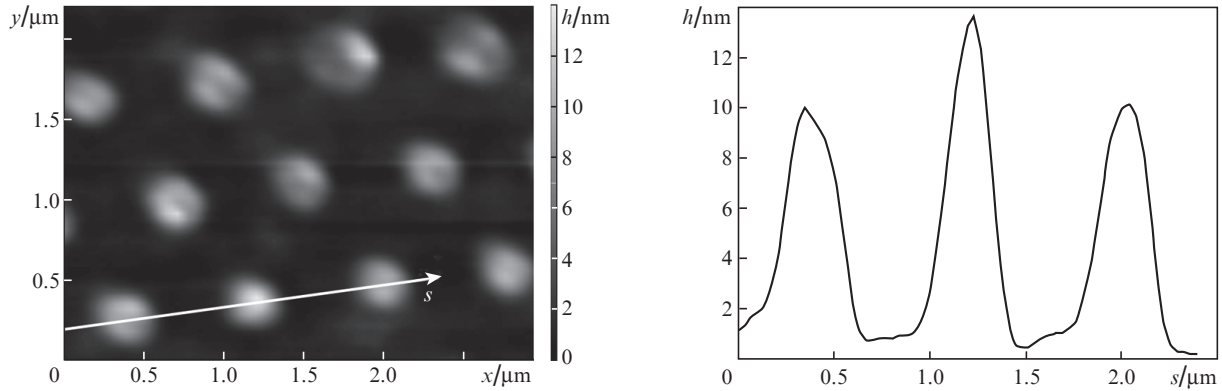


Figure 6. Structures (bumps) obtained on a glass substrate by exposure to a single bichromatic femtosecond pulse through a microspheres array. Shown in the right panel is the height profile along line s in the grey-scale map of the height (h) distribution above the xy plane (atomic force microscope image).

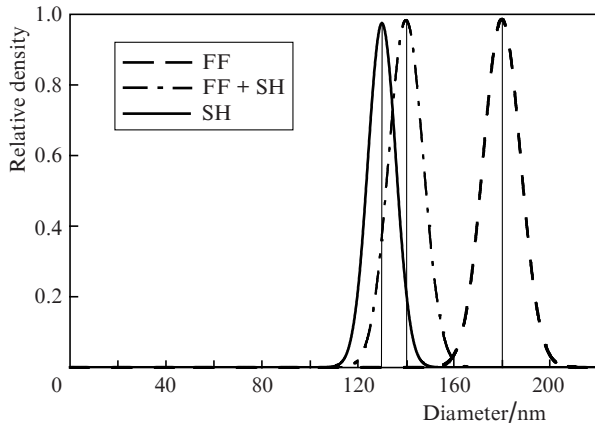


Figure 7. Ablation pit size (full width at half maximum) distributions on PMMA at the structuring threshold. The data were obtained by analysing 30 profiles for each type of pulse (FF, SH and FF + SH).

modern literature. According to earlier findings [13], the SH is more efficient in the case of multiphoton ionisation than is the fundamental, which is in turn efficient when impact ionisation increases the number of free electrons. As shown above, the SH is better focused by an array of spheres. This accounts for the decrease in the modification threshold and the transverse size of the structures when the bichromatic irradiation is used.

The question of whether impact ionisation contributes to free carrier generation requires separate discussion. In self-similar avalanche mode, impact ionisation ensures an electron multiplication factor $\sim \exp(f/f_0)$, where f is the pulse energy density (laser fluence) and f_0 is a characteristic fluence for impact ionisation.

As pointed out above, the threshold power density at the fundamental frequency for the removal of the spheres by a double-frequency pulse was $5 \times 10^{11} \text{ W cm}^{-2}$.

It follows from Fig. 2 that, with allowance for the electrodynamic interaction in an array of spheres, it ensures an increase in intensity by about a factor of 5. Given that structuring occurs at pulse energies about 15% higher than the sphere removal threshold and that the pulse duration in our experiments was 50 fs, we find the threshold fluence for structuring: $f \approx 150 \text{ mJ cm}^{-2}$.

The amorphous polymer PMMA used in our experiments has a large free volume. Free carriers are generated in it via ionisation of its molecules. The conduction band electrons are merely free electrons, i.e. the effective electron mass is equal to the free electron mass.

Solving the rate equation for the conduction electron energy distribution using the Fokker–Planck equation in a double flux approximation (see details e.g. in Ref. [13]) we obtain

$$f_0 = \frac{3}{4\pi 2.38} \frac{m}{e^2} \frac{\omega^2 + \nu^2}{\nu} \frac{c}{n_\omega} E_i.$$

Here, m is the electron mass, e is the electron charge, $\omega = 2.36 \times 10^{15} \text{ s}^{-1}$ is the laser fundamental frequency, ν is the collision frequency, c is the speed of light, n_ω is the index of refraction, and E_i is the ionisation energy. Taking m equal to the free electron mass, $n_\omega = 1.5$, $E_i = 10 \text{ eV}$ and $\nu = 10^{15} \text{ s}^{-1}$, we obtain $f_0 = 70 \text{ mJ cm}^{-2}$. The collision frequency $\nu = 10^{15} \text{ s}^{-1}$ corresponds to an electron free path of 1 nm and kinetic energy of 3 eV.

Thus, f exceeds f_0 by about a factor of 2 and impact ionisation ensures free electron multiplication and increases the electron concentration by about one order of magnitude. The above estimates confirm that impact ionisation can be essential under the experimental conditions of this study.

Electrodynamic calculation results suggest that, for efficient formation of a near-field maximum, the polystyrene sphere diameter should be at least about half the wavelength. As seen in Fig. 2, the structuring density is highest and the width of the field maximum is smallest at a wavelength of the order of the sphere diameter.

Our experimental data demonstrate that the possibility of localising the laser modification region under bichromatic irradiation is determined by the SH intensity distribution. This means that we can use spheres with a diameter close to the wavelength corresponding to the SH rather than to the FF.

Figure 8 shows intensity distributions in the case of focusing by an array of spheres with a diameter half that above. It is seen that the SH is well focused by 400-nm-diameter spheres, whereas FF radiation is not focused and passes with negligible attenuation. Thus, using smaller spheres, we can reduce the spacing between ablation craters by at least a factor of 2. We plan to carry out such experiments in the nearest

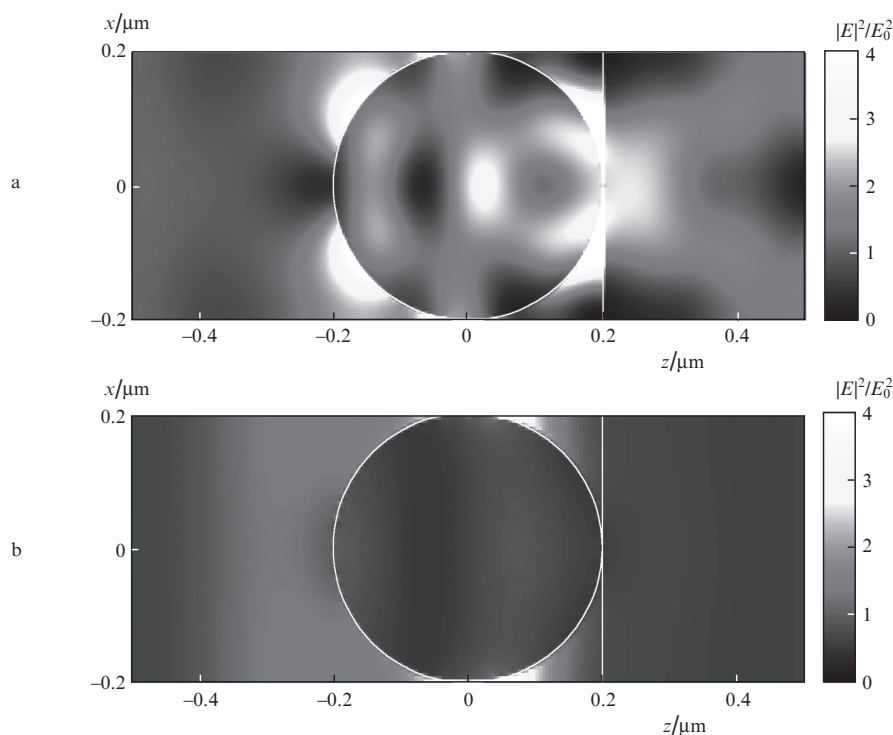


Figure 8. $|E|^2$ distributions near 400-nm-diameter polystyrene spheres ($n = 1.59$) in an infinite monolayer on a glass substrate ($n = 1.46$) under the action of normally incident plane waves with $\lambda =$ (a) 400 and (b) 800 nm, linearly polarised along the x coordinate. The distributions are normalised to the field in the incident wave.

future. In addition, we plan to optimise the temporal shape of bichromatic pulses. The SH pulse should precede the FF pulse and, to further reduce the multiphoton ionisation efficiency at the fundamental frequency, we plan to stretch the FF pulse.

6. Conclusions

We have considered the surface nanostructuring of solids, such as polymers and glasses, by femtosecond laser pulses using a colloidal particle array as a focusing system and assessed the effect of intense femtosecond laser radiation in single-shot mode. The fundamental frequency of such lasers, typified by the Ti:sapphire laser, with a wavelength of ~ 800 nm, lies in the near-IR spectral region. The present experimental data demonstrate that, in the case of polymers, partial conversion of the laser pulse energy into the SH using a non-linear crystal, i.e. the use of bichromatic pulses, reduces the laser nanostructuring threshold by about a factor of 2 and decreases the transverse size of elementary structures, e.g. ablation craters. The crater radius in the case of bichromatic pulses (less than 100 nm) was 30% smaller than that in the case of FF pulses. In our experiments, a pulse energy of 1.7 mJ was used, and up to 5% of the FF pulse energy was converted to the SH. The samples used had the form of arrays of 1- μm -diameter polystyrene spheres on poly(methyl methacrylate) or glass substrates.

At intensities above 10^{12} W cm $^{-2}$, which corresponds to the modification threshold, surface modification (ablation and swelling) occurs through free carrier generation. In this process, the SH is more efficient for multiphoton ionisation, i.e. it produces conduction band electrons more efficiently than does FF radiation, whereas the latter is more efficient in

impact ionisation, i.e. it adequately ‘multiplies’ electrons. Thus, the SH produces seed electrons, whereas the fundamental ensures an energy effect. We have shown that the SH is better focused by colloidal particle arrays than is FF radiation. In data analysis, we took into account that a close-packed microsphere array cannot be treated as a system of independent microlenses. In such a system, a significant role may be played by light rescattering within the layer. Since seed SH radiation is better focused by a microparticle array, the near-threshold size of the laser modification region for a bichromatic beam will correspond to that for the SH. Basically, we have proposed a simple approach for improving the sensitivity and resolving power of one of the main methods for surface nanostructuring by femtosecond laser pulses.

Acknowledgements. This work was supported by the Presidium of the Russian Academy of Sciences (Programme No. 13: Extreme Light Fields and Their Applications).

We also acknowledge the support from the RF Ministry of Education and Science, the Russian Foundation for Basic Research (Grant Nos 13-02-97075-a povolzhie and 13-02-12433-ofi_m2) and the Presidium of the Russian Academy of Sciences (Programme No. 24: Fundamental Issues in the Technology of Nanostructures and Nanomaterials).

References

1. Luk'yanchuk B.S., Wang Z.B., Song W.D., Hong M.H. *Appl. Phys., Mater. Sci. Process.*, **79**, 747 (2004).
2. Langer G., Brodoceanu D., Bäuerle D. *Appl. Phys. Lett.*, **89**, 261104 (2006).
3. Wu W., Katsnelson A., Memis O.G., Mohseni H. *Nanotechnology*, **18**, 485302 (2007).

4. Khan A., Wang Z.B., Sheikh M.A., Whitehead D.J., Li L. *Appl. Surf. Sci.*, **258**, 774 (2011).
5. Chong T.C., Hong M.H., Shi L.P. *Laser Photonics Rev.*, **4**, 123 (2010).
6. Pikulin A., Bityurin N., Langer G., Brodoceanu D., Bäuerle D. *Appl. Phys. Lett.*, **91**, 191106 (2007).
7. Pikulin A., Afanasiev A., Agareva N., Alexandrov A.P., Bredikhin V., Bityurin N. *Opt. Express*, **20**, 9052 (2012).
8. Bityurin N.M. *Kvantovaya Elektron.*, **40**, 955 (2010) [*Quantum Electron.*, **40**, 955 (2010)].
9. Bityurin N., Afanasiev A., Bredikhin V., Alexandrov A., Agareva N., Pikulin A., Ilyakov I., Shishkin B., Akhmedzhanov R. *Opt. Express*, **21**, 21485 (2013).
10. Englert L., Rethfeld B., Haag L., Wollenhaupt M., Sarpe-Tudoran C., Baumert T. *Opt. Express*, **15**, 17855 (2007).
11. Mauclair C., Zamfirescu M., Colombier J. P., Cheng G., Mishchik K., Audouard E., Stoian R. *Opt. Express*, **20**, 12997 (2012).
12. Englert L., Wollenhaupt M., Sarpe C., Otto D., Baumert T. *J. Laser Appl.*, **24**, 042002 (2012).
13. Bityurin N., Kuznetsov A. *J. Appl. Phys.*, **93**, 1567 (2003).
14. Wang Z.B., Guo W., Luk'yanchuk B., Whitehead D.J., Li L., Liu Z. *J. Laser Micro/Nanoeng.*, **3**, 14 (2008).
15. Langmuir I.J. *J. Chem. Phys.*, **6**, 873 (1938).
16. Langmuir I.J. *Am. Chem. Soc.*, **39**, 1848 (1917).
17. Blodgett K.B. *Am. Chem. Soc.*, **57**, 1007 (1935).
18. Xiaozhou Y., Qi L. *Nano Today*, **6**, 608 (2011).
19. Luk'anchuk B. (Ed.). *Laser Cleaning* (World Scientific, 2002).